

Senior Thesis

An Examination of the Variation in the
concentration of Fe, Ti, and Mn within
the Different Size Fractions of Till
South of the Sanford Hill Titanomagnetite
Deposit, Essex County N.Y.

by

Kent Whiting

1988

Submitted as partial fulfillment of the
requirements for the degree of Bachelor
in Geology and Mineralogy at the Ohio
State University.

Autumn Quarter 1988

HONORABLE MENTION

1988

Approved by:

Gunter Faure
Dr. Gunter Faure

Table of Contents

Abstract.....	1
Introduction.....	2
Choice of Locality.....	3
Geologic Setting and Mineralogy of the Deposit.....	4
Fieldwork.....	10
Laboratory Procedure.....	13
Results.....	17
Conclusions.....	31

Abstract

The variation in the concentration of Fe, Ti, and Mn with distance for the -60+120 fraction of till south of the Sanford Hill Ore Body is similar to that demonstrated for the crystalline clasts south of the Canadian Shield. Near the deposit the concentrations decrease sharply with distance until reaching a transition distance where the concentrations stabilize. These trends are known as the "head" and "tail" of the anomaly respectively. The head of the Sanford Hill anomaly is the region in which the concentrations of Ti, Fe, and Mn in the -60+120 mesh fractions decrease exponentially with distance. Analyses of different size fractions show evidence for differential grinding of plagioclase and magnetite-ilmenite. Therefore, bulk till samples should be used in order to average out the relative changes in the mineral composition of the grain size fractions with distance of glacial transport. Within the tail of the anomaly the transport mechanism of the ore material is englacial. These grains migrate from the interior of the ice to the zone of active grinding at the base of the glacier due to melting.

Introduction

While the use of ore boulders as a guide to prospecting for mineral deposits is not new, the use of the finer size fractions has only recently been studied. (Dreimanis 1971, Kauranne 1976 etc.) The main advantage demonstrated in these investigations is the low sampling density required for regional prospecting when sampling the finer material. Once an area is found to have anomolous concentrations of the desired mineral or element, the next objective is usually to locate the axis of the "glacial fan" by taking samples perpendicular to the ice flow direction. This is where most studies stop. Few investigators have studied in detail how the abundance of ore material in till varies along the axis of the fan. If a consistent pattern can be found for the different size fractions of till, then a universal technique for predicting the locations of buried ore deposits may be developed. This method would enable geochemists to determine not only the direction to a deposit but also the approximate distance. The groundwork for this type of investigation was established by Shilts in 1973 who found that there are two distinctive zones along the fan which he termed the "head" and the "tail". The head is the area closest to the deposit and is recognized by the sharp decline in the abundance of indicator pebbles within the till. The tail on the other hand is the zone in which the abundances stabalize to a relatively constant value. An important advance of this study was the discovery by Strobel and Faure (1987) that in the head the abundances decrease exponentially, while in the tail the decrease is linear. In theory, if the head of the anomaly can be found, then the distance to the deposit can be calculated by a method suggested by Strobel and Faure (1987). At

present, this relationship is valid only for the clast-sized material, due to the fact that sand-sized material was not considered in the study. There is no reason to believe, however, that this should not hold true for the finer size fractions if a head and tail can be shown to exist, especially if one can consider sand-sized material to be "microclasts".

In this study I will attempt to show that this is indeed the case. If the advantages of sampling sand-sized till can be combined with a knowledge of how the ore material is distributed down ice from a deposit, then a useful exploration tool may be developed. A second objective of this study will be to determine what size fractions should be sampled for a particular ore type. This would enable geochemists to process till samples more efficiently, since only one analysis would be necessary for each sample.

Choice of Locality

The most important conditions considered when choosing a locality for this study were as follows: the mineral deposit should be compositionally distinctive from the surrounding rock types, have been at the surface during Pleistocene glaciation, and contain elements that can be detected using the analytical tools available at O.S.U.

The Sanford Hill iron-titanium deposit of north-eastern New York was found to meet these qualifications (See figure 1). In addition, this deposit is in an area where the till is exposed sufficiently so that simple and inexpensive sampling methods could be employed.

Geologic Setting and Mineralogy of the Deposit

The Sanford Hill deposit is one of four titaniferous magnetite deposits located in the Sanford Lake area of Essex County New York. These deposits are within the Adirondack anorthosite massif, which is of Proterozoic age. This massif is within the Grenville Series of granulite facies metamorphic rocks. These rocks were produced under conditions of high temperature and pressure and have been interpreted to be the core material of nappes and domes formed prior to the Grenville orogeny. (Walton and DeWard 1962) The rocks were later uplifted and eroded, exposing the high grade rocks at the surface. This uplift occurred mainly due to the Grenville orogeny, although the later Taconic and Appalachian uplifts to the east undoubtedly affected the previously established fault system in the area. (Anonymous 1967). There are two types of anorthosite within the massif, the Marcy, which is the most abundant, and the Whiteface which is found predominantly along the border of the massif. The Marcy type is a greenish rock composed of labradorite feldspar with fine inclusions of ferromagnesian minerals such as pyroxene, hornblende and biotite. The Whiteface anorthosite is light gray in color and is composed of andesine feldspar and ferromagnesian minerals. The Marcy Type is more common in the Sanford Lake area than the Whiteface type, and the contact between the two types is usually gradational. The anorthosites form a sharp contact with gabbro, which grades into titaniferous magnetite as the deposit is approached. (Anonymous 1967) Gabbro forms an envelope around the Sanford hill deposit, and is composed of clinopyroxene, plagioclase and hornblende with lesser amounts of garnet, magnetite and ilmenite (Kays 1965). The ore is composed of magnetite grains within

an ilmenite matrix. In addition, Kays (1965) found that ulvospinel (Fe_2TiO_4) occurs in a fine network within magnetite grains. The ulvospinel content was found to be on the order of 3.4 per cent. On the average, the ratio of Fe to Ti is 2 to 1 (Anonymous 1967). The ore of the Sanford Hill deposit and the South Extension occur as lenses along a fault that strikes N30E and dips approximately 45 NW. (See Fig. 2.1)

During Pleistocene time the area was glaciated, which resulted in scouring of the bedrock and deposition of glacial deposits. The Sanford Lake area is well within the realm of the Labrador ice sheet. The number of times the ice advanced and retreated is unknown, presumably the last advance erased any evidence of previous advances. The principle glacial deposits are till and outwash. The till deposits are found mainly on the hillsides while the outwash deposits are concentrated at lower elevations along the Hudson River valley, which was a major drainage for the ice sheet.

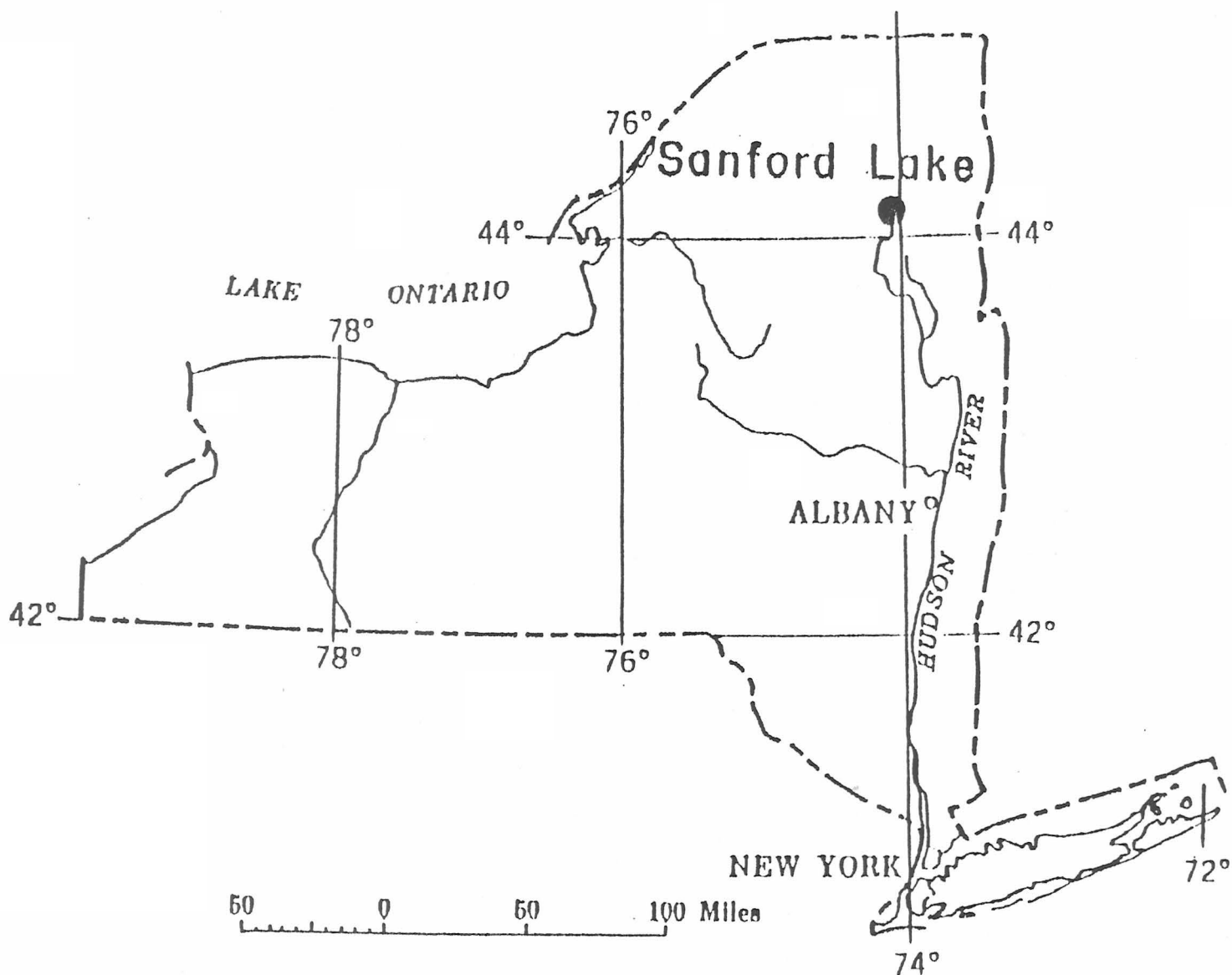


Figure 1 Location of the study area in the central highlands of the Adirondack anorthosite massif of north-eastern New York. The Sanford Hill ore body is one of four titanomagnetite deposits in the Sanford Lake region of Essex Co. N.Y. After Anonymous 1987.

Figure 2. Map of the deposits of the Sanford Lake area showing the locations of the various till samples. The estimated locations of the Pleistocene outcrop is indicated by an "x".

FIG 2

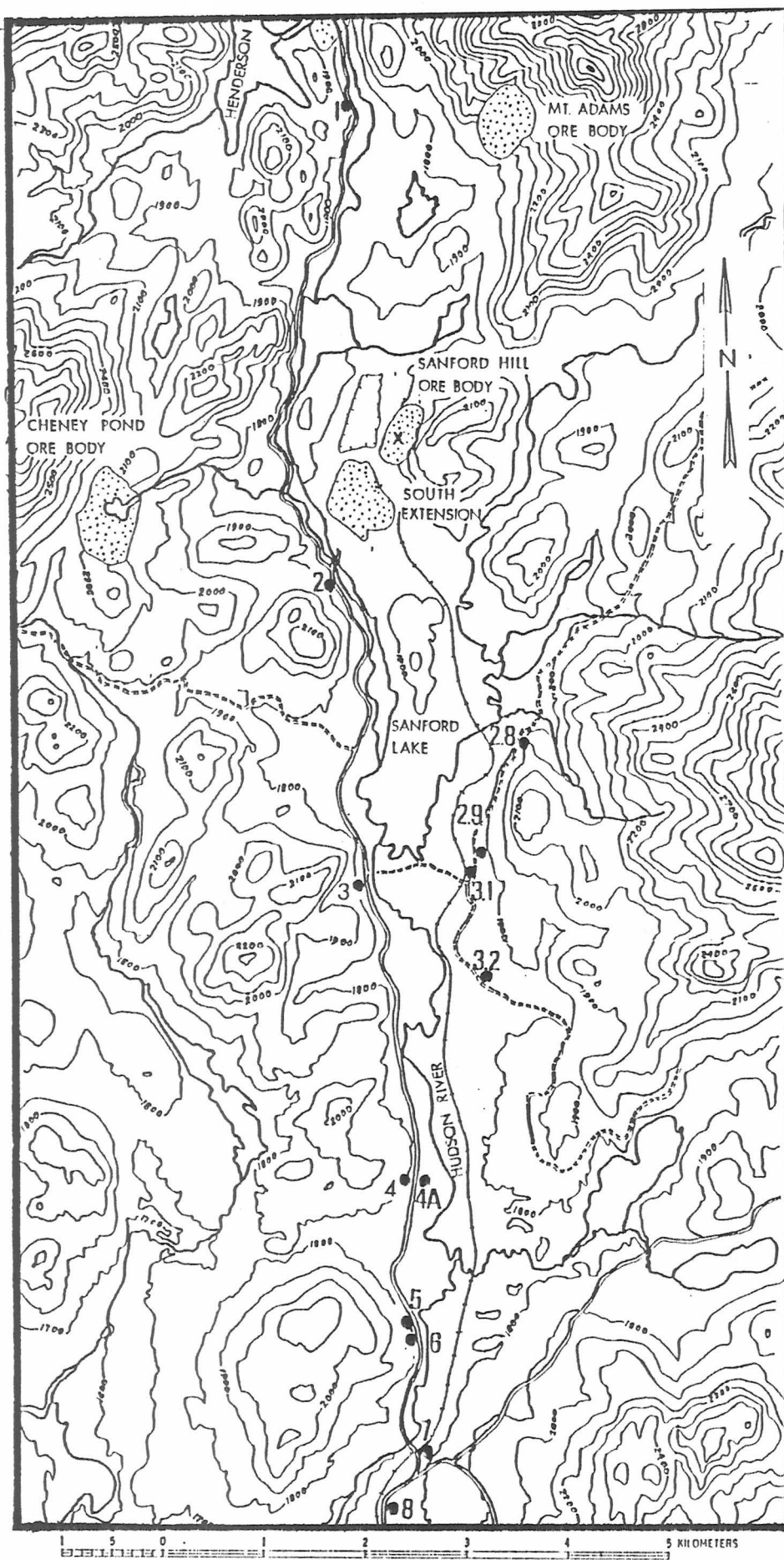
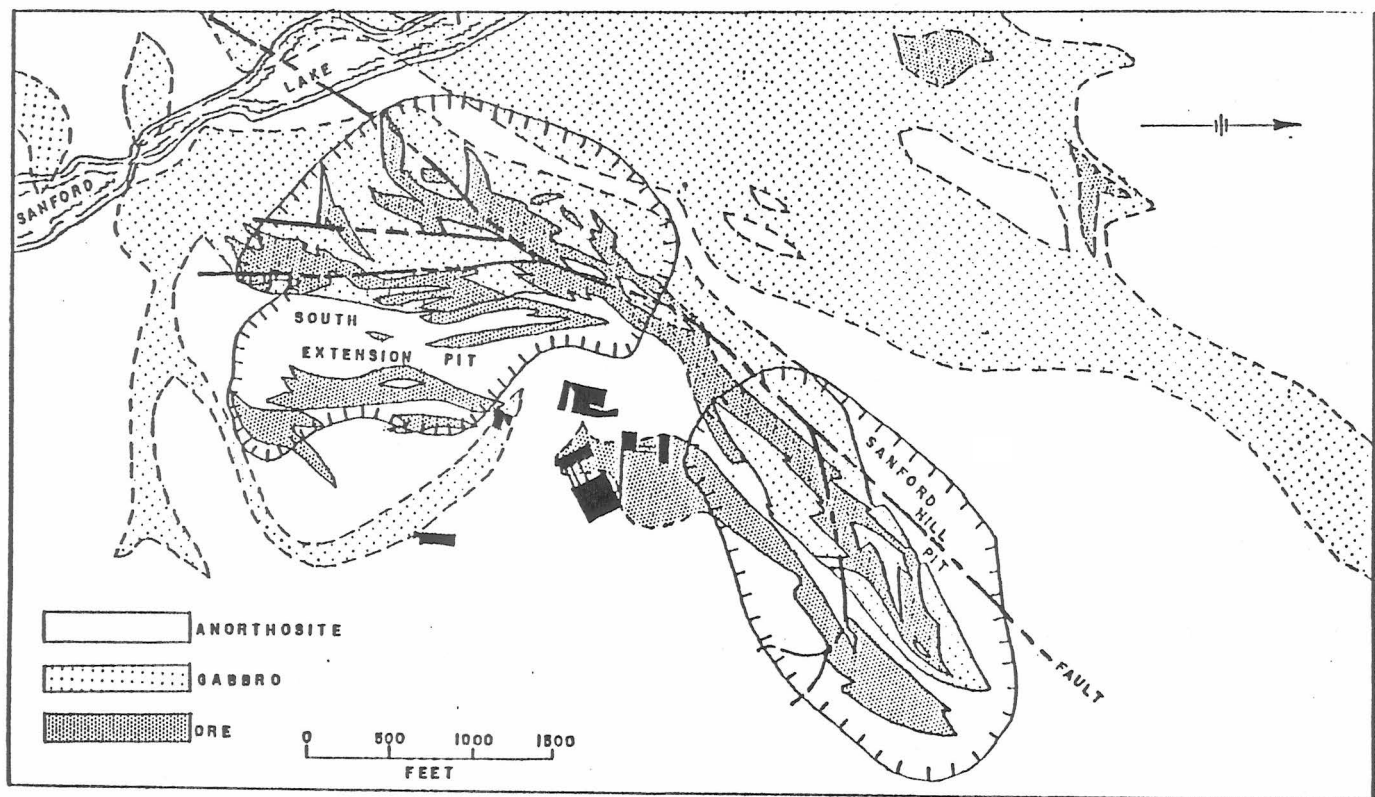


Figure 2-1. Bedrock geology of the Sanford Hill and South Extension ore bodies showing the extent of the mining operations in 1967 and the distribution of the ore lenses. After anonymous 1967.



Fieldwork

Fourteen samples of till were collected on June 11, 1988, along a 13 Km traverse parallel to the direction of ice flow, using a 15-minute topographic map. One sample was collected north of the Sanford Hill deposit in order to provide a background value to which the expected geochemical anomaly in the south could be compared. The collecting was facilitated by the existence of a 13 Km paved road, which was built by the National Lead Company in 1941 in order to link the mining operations and the village of Tahawus to the nearest State Highway. This road runs north-south, which is roughly parallel to the direction of flow of the Labrador ice sheet. (See Figure 2). Several samples were taken where the road traversed the bases of hills along the western edge of the Hudson River valley which exposed basal till. In addition to the road, there is a railine running north-south along the eastern edge of the Valley, which was also built by National Lead, in order to link the mine to the railhead at Northcreek 30 miles away.

The area had changed considerably since publication of the topographic map in 1953 because of stripping and mining operations of the "South Extension" of the Sanford Ore body. Not only was the pit greatly enlarged compared to 1953, but large piles of waste rock had been dumped on some of the best till outcrop sites. The volume of this material was so large that it buried part of Tahawas, which is now a ghost town.

The loss of accessible sites caused by dumping of mine waste was compounded by the presence of a thick cover of organic debris.

Apparently in the past 47 years since the road was built plant debris produced by the dense forest in the area has crept downslope to cover former till exposures along the road. In addition, the railroad was situated over outwash deposits, which further limited my collecting possibilities. The outwash deposits were easily recognized due to the high degree of sorting, large clast size, and loose packing of the material. In spite of these difficulties, I was able to collect samples by digging near the edges of the slumps of organic matter. Nevertheless, three out of the ten samples collected along the road deviated in some way from the characteristic basal till desired for this study.

I was able to collect an additional four samples along a gravel road just east of the railline. (See Figure 2) This road was built above the outwash deposits in an area where till had been plastered to the side of the valley wall. This road had better outcrops than the paved road to the west, but unfortunately its course deviated from the ideal north-south course and merged east along Dudley Creek at its northern end, while the southern end curved around the North Mountains and headed northeast along Perch Pond. There was, however, a 3 Km section along this road that ran parallel to the Hudson River Valley, and provided a sufficient number of samples to complete my field work.

The characteristic basal till mentioned above consists of a hardpacked mixture of light gray and black colored grains, presumably composed of plagioclase and magnetite, respectively. Sand sized grains are by far the most abundant, although the range is from very fine grained sand to fist-sized clasts. The light gray grains are angular and exhibit good cleavage, while the black grains are subangular and

lack cleavage. The various grains of different sizes and composition are well mixed and evenly distributed throughout the till, producing a mixture resembling salt and pepper. In general, the clasts are spherical, and therefore they are not useful in verifying the ice flow direction by the alignment of their axes. The till is oxidized to a depth of about 46 cm. This oxidized layer is in general of uniform thickness and is reddish brown in color. The contact between the oxidized and fresh till is fairly sharp to gradational.

As mentioned above, three samples deviate from this description, they are as follows:

Sample 3 - While the basal till was oxidized to approximately 46 cm, the material from which this sample was collected was oxidized to at least 80 cm. Therefore I collected the oxidized material from a depth of about 90 cm. In addition, there were more rusty clasts at this site than elsewhere.

Sample 4 - This material was exposed on a high bank of a small creek. In general, the grainsize was smaller than the characteristic basal till, and was better sorted.

Sample 66- This material was not nearly as hardpacked as the basal till and was better sorted. The sharp contact between this fine gray material and the more till-like oxidized material above led me to believe that this was an iron poor sand lens within oxidized basal till.

The collecting procedure consisted of digging a pit through the organic cover and oxidized layer to the fresh salt and pepper till below, which was only rarely exposed in outcrop. This was done using a

small entrenching tool. Every attempt was made to collect unoxidized till in order to eliminate the possibility of compositional changes brought about by leaching. Approximately 500 grams of material was collected at each site and placed into a small cloth bag which was then clearly marked. In addition, the collecting sites were marked on a topographic map shown in Figure 2.

Laboratory Procedure

In order to determine the amount of ore material present within each sample, a chemical analysis of the till was necessary. Since this study is concerned with only the smaller grain sizes, a physical count of the grains would be tedious and impractical. Thus, the following procedure was employed:

1. The samples were weighed on a double beam balance in grams, and the -60 +120 mesh fraction was recovered by sieving.
2. The -60 +120 fractions were weighed, and 3.5 gram aliquants were placed in a mechanical mortar and ground to a fine powder.
3. The powdered samples were pressed into pellets composed of 3g of till and 6 grams of boric acid as a backing.
4. The pellets were then analyzed for iron, titanium, manganese, and chromium using x-ray fluorescence spectrometry. (Diano Corp. Model XRD-6. equipped with a Mo-target x-ray tube and a L:F 220 analyzing crystal.)

The XRF machine was calibrated by analyzing USGS rock standards W-1, G-2, AGV-1 and BCR-1. The known concentrations of Ti, Mn, Fe, and Cr were then plotted versus the ratio of net x-ray intensity of the K-alpha line of each element divided by the total counting rate of the

Compton-scattered Mo K-alpha peak. From these plots the following linear equations were derived:

$$(1) \text{Fe}_2\text{O}_3 \text{ (wt. \%)} = 1.4522 (\text{Fe/Mo}) + 0.735$$

$$(2) \text{Ti (ppm)} = 85845.54 (\text{Ti/Mo}) - 189.173$$

$$(3) \text{Mn (ppm)} = 16857.338 (\text{Mn/Mo}) + 92.636$$

$$(4) \text{Cr (ppm)} = 27523.911 (\text{Cr/Mo}) - 7.2776$$

The measured Ti/Mo, Fe/Mo, Mn/Mo and Cr/Mo values of the till samples were then substituted into the appropriate calibration equations to obtain the desired concentrations of the four elements. All samples were analyzed in triplicate. In order to monitor the accuracy of the analysis, AGV-1 was analyzed with the unknowns and the measured concentrations were adjusted using a correction factor (f) which was obtained in the following way:

$$f = \text{AGV-1 (standard)} / \text{AGV-1 (measured)}$$

The correction factors and corrected concentrations are shown in appendix A. The mean concentrations (M) and standard deviation (σ) were calculated, and are summarized in Tables 1-1 and 1-2.

Table 1-1 Average Fe and Ti concentrations of -60+120 mesh fractions of till from the Sanford Lake area, N.Y.

<u>Sample Number</u>	<u>Distance from the Sanford Hill Ore Body. (Km)</u>	<u># Fe concentration Wt. %</u>	<u>Ti concentration, ppm $\pm \text{ } \dagger$</u>
1*	-3.3	6.03 \pm .02	21,922 \pm 340
2	1.5	7.40 \pm .03	29,733 \pm 750
2.8	3.1	4.59 \pm .02	12,812 \pm 312
2.9	4.2	4.31 \pm .01	13,051 \pm 121
3.0	4.5	12.64 \pm .03	37,480 \pm 557
3.1	4.4	3.48 \pm .01	7,524 \pm 145
3.2	5.4	4.62 \pm .02	12,722 \pm 543
4	7.4	5.19 \pm .02	16,306 \pm 308
4A	7.4	4.01 \pm .02	10,399 \pm 48
5	8.8	5.56 \pm .01	15,598 \pm 261
6R	8.9	5.03 \pm .01	14,285 \pm 342
6G	8.9	3.17 \pm .01	6,297 \pm 207
7	10.0	6.35 \pm .02	23,089 \pm 253
8	10.6	5.27 \pm .01	16,331 \pm 210

Note - Fe_2O_3 Wt.% was converted to Fe Wt.%.

* Note - Since sample 1 was collected north of the deposit it was assigned a negative distance.

† Note - $\text{ } \dagger$ is equal to the standard deviation from the mean.

Table 1-2 Average Cr and Mn concentrations of -60+120 mesh fractions of till from the Sanford Lake area N.Y.

<u>Sample Number</u>	<u>Distance from the Sanford Hill Ore Body (Km)</u>	<u>* Cr concentration ppm \pm 6</u>	<u>Mn concentration ppm \pm 6</u>
1	-3.3	43 \pm 11	791 \pm 9
2	1.5	59 \pm 2	1032 \pm 15
2.8	3.1	76 \pm 7	663 \pm 17
2.9	4.2	53 \pm 8	681 \pm 20
3.0	4.5	74 \pm 7	2085 \pm 7
3.1	4.4	22 \pm 9	541 \pm 36
3.2	5.4	44 \pm 9	680 \pm 18
4	7.4	54 \pm 9	774 \pm 40
4A	7.4	37 \pm 8	630 \pm 25
5	8.8	55 \pm 8	897 \pm 7
6R	8.9	64 \pm 3	681 \pm 34
6G	8.9	21 \pm 10	498 \pm 27
7	10.0	49 \pm 14	920 \pm 3
8	10.6	26 \pm 5	817 \pm 32

* Note - Cr values were not corrected, since the value of 12 ppm for AGV-1 is close to the detection limit using XRF.

Results

The distances reported in tables 1-1 and 1-2 were measured from a point presumed to be near the south edge of the original outcrop. This reference point is indicated by an "x" in figure 2. Notice that the stippled pattern in this figure represents the extent of the mine, not the Pleistocene outcrop.

In order to determine how the concentration of ore material within the till changes with the distance from the source, a plot of distance vs. concentration was constructed for each element. (See figures 3, 4, and 5)*. The variations in the concentrations of Ti, Fe and Mn with distance show a similar pattern to the abundance of crystalline clasts with distance in the Dummer Moraine of Ontario (Strobel and Faure 1987). With the exception of sample 3, which may not be basal till, sample 2 showed the highest concentration of ore minerals. From sample 2 to sample 2.8 the concentration drops sharply, while between samples 2.8 and 8 the values remain fairly stable. These two intervals can be interpreted to be the "head" and the "tail" of the anomaly. According to Strobel and Faure the concentrations within the head should decrease with distance according to the following relationship

$$\ln A = \ln A_0 - KD \quad (5)$$

Where A is the abundance of material at a distance (D) from the source, A_0 is the initial abundance of ore material and K is the "transport constant". Since equation 5 is a linear plot of $\ln A$ vs D, samples within the head should yield a straight line.

*Note - A plot of chromium vs distance was not included because the accuracy of the analysis was not great enough to resolve small concentration variations so close to the detection limit.

Figures 3, 4, and 5 Fe, Ti, and Mn concentrations in the -60+120 fraction of till vs the distance from the Sanford Hill Ore deposit. Positive distances represent samples collected south of the deposit, while negative values are to the north. The solid dots represent characteristic basal till while the 'X"s denote the "questionable" samples described in the text.

Figures 3.1, 4.1, and 5.1 Natural logarithm of the concentration of Fe, Ti, and Mn vs distance from the Sanford Hill deposit.

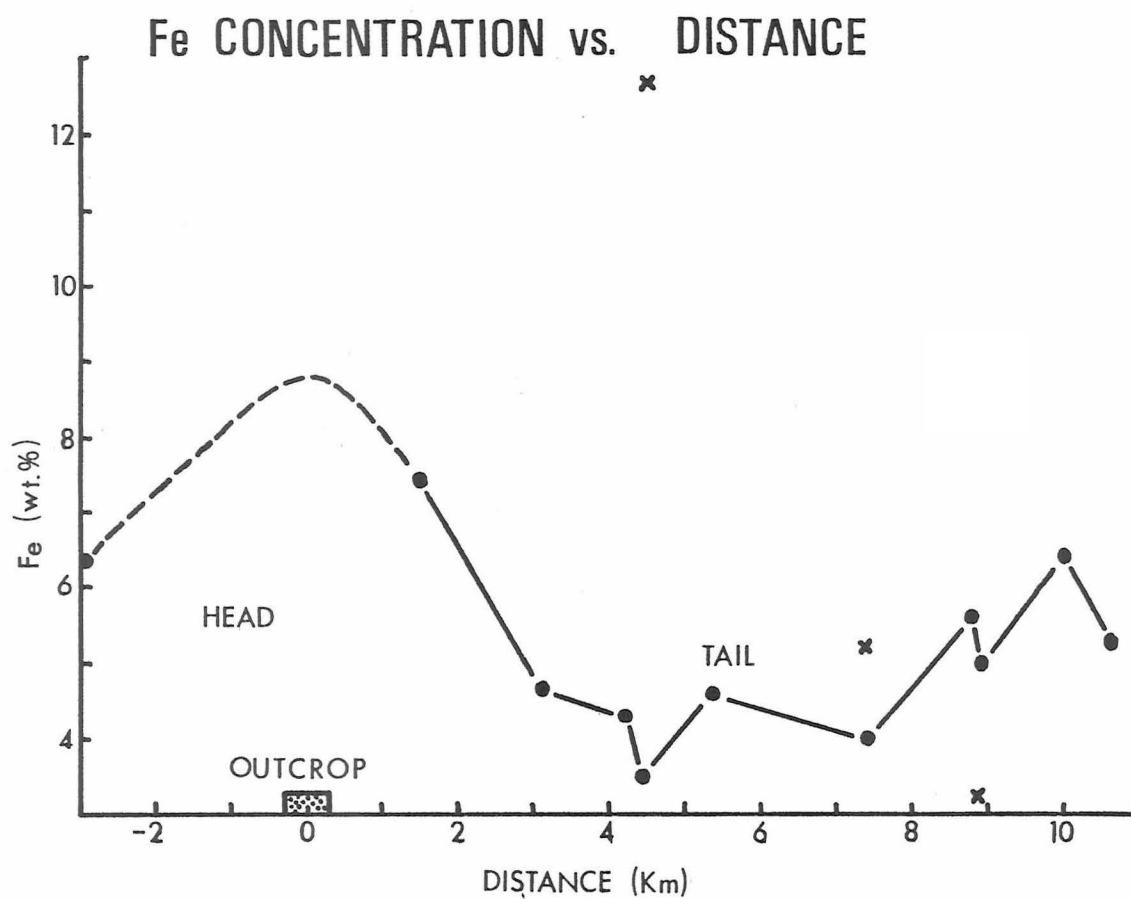


FIG. 3

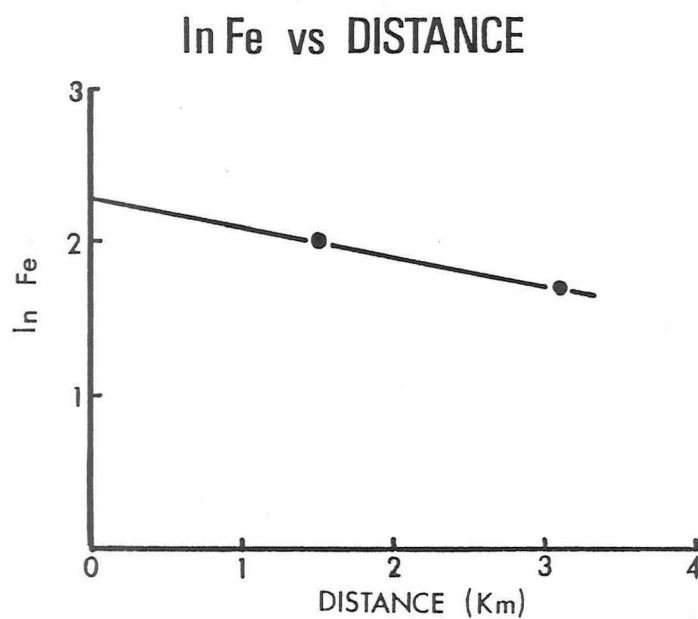


FIG. 3.1

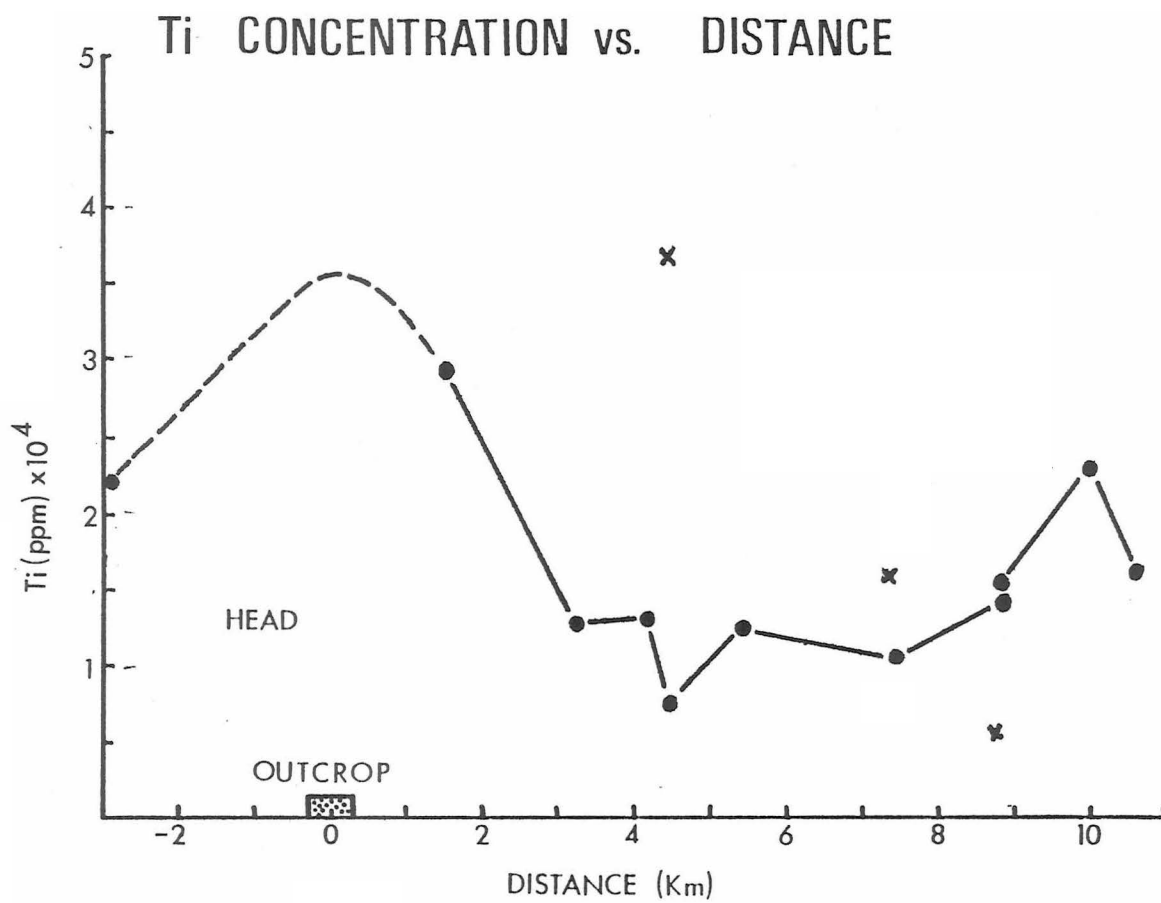


FIG. 4

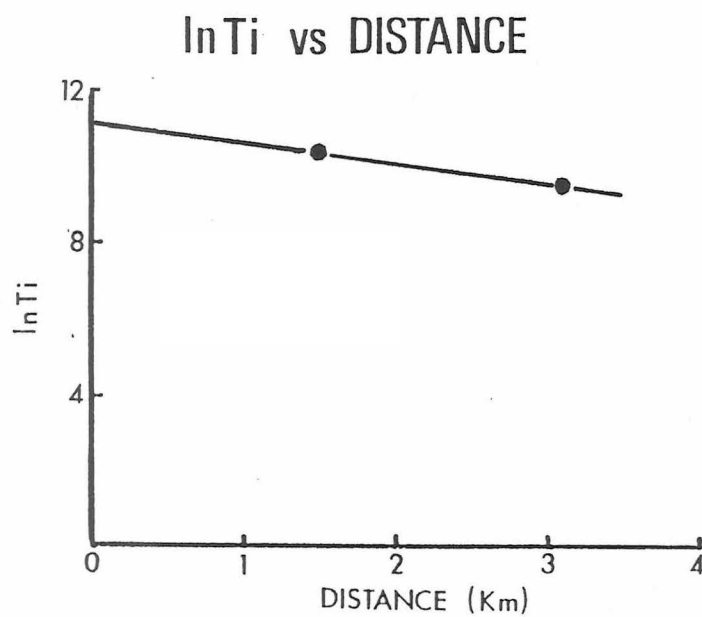


FIG. 4.1

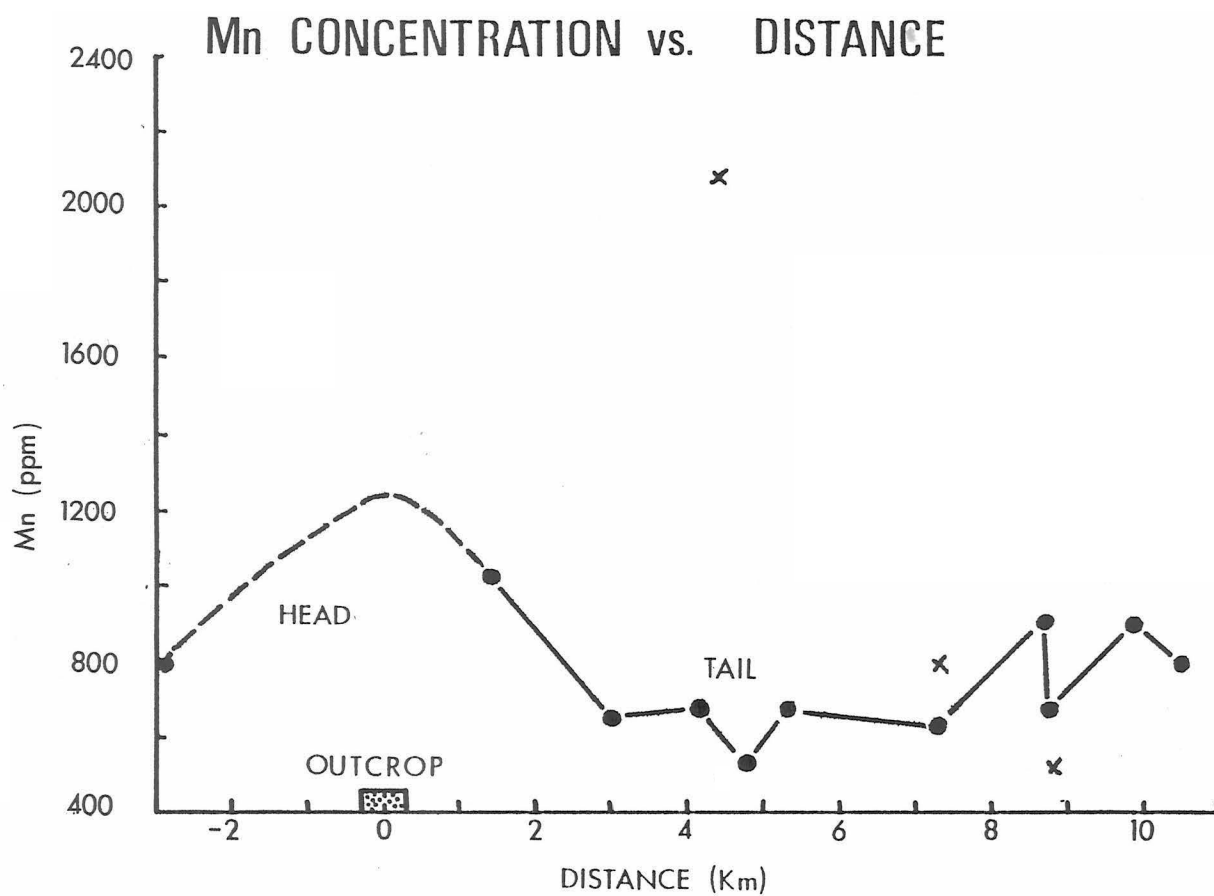


FIG.5

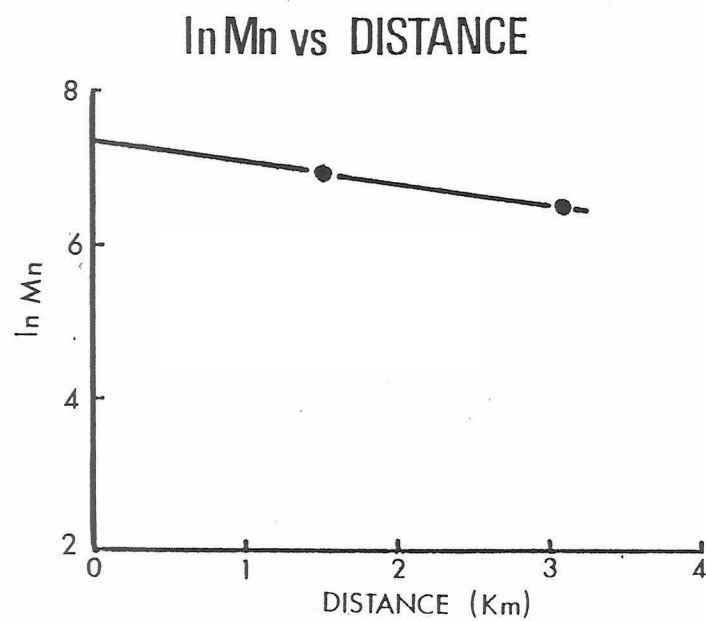


FIG. 5.1

Unfortunately, I was only able to obtain two samples from within the "head" section due to a lack of outcrops as discussed earlier. A plot of $\ln A$ vs D for each element is shown in figures 3.1, 4.1, and 5.1. The fact that a straight line was obtained obviously does not prove that an exponential relationship exists, since any two points yield a straight line. The reason the figures were included is, if, based on the general form of the concentration vs D plots samples 2 and 2.8 can be assumed to be part of the head, then figures 3.1 through 5.1 can be used to generate further data. For example, the intercept value on the $\ln A$ axis yields $\ln A_0$, and the slope of the line yields $-K$. K can be used to determine the transport half-distance ($D_{1/2}$) by the following equation: (Strobel & Faure, 1987)

$$D_{1/2} = \frac{\ln 2}{K} \quad (6)$$

The half-distance is the distance at which A is reduced by one half. $D_{1/2}$ is a useful value that allows one to assign a numerical value to the way in which the elements decrease relative to the source. Values for D and A are shown in table 2.

Table 2 Transport constant, half-distance and initial concentration values for the ore related elements in the -60+120 mesh fractions

<u>Element</u>	<u>k</u>	<u>D 1/2</u>	<u>A₀</u>
Ti	.52	1.3 km	36,313 ppm
Fe	.25	2.8 km	9.97%
Mn	.26	2.7 km	1,480 ppm

From Table 2, it appears as though Ti is more easily ground than Fe and Mn, since its half distance is only about one half that of Fe and Mn. In order to determine if this is true for other size fractions, the

-18+35, -35+60, -120+200 and -200 mesh fractions were analyzed for samples 2 and 2.8, using the same laboratory procedure as before. The averaged values are shown in Table 3-1, while the raw values and correction factors are listed in Appendix B.

Table 3-1 Average Fe, Ti and Mn concentrations for each size fraction of till from the Sanford Lake area N.Y.

<u>Size Fraction</u>	<u>Fe (wt%)</u>	<u>Sample 2 Ti (ppm)</u>	<u>Mn (ppm)</u>
- 18+35	3.86±.13	8253±85	498± 9
- 35+60	5.11±.01	13649±46	564± 6
- 60+120	7.40±.03	29733±749	1032±15
-120+200	6.61±.02	12683± 93	1059± 34
-200	5.91±.02	10566±187	974± 12
Sample 2.8			
- 18+35	5.78±.03	14537±232	665± 10
- 35+60	8.46±.08	22355±373	801± 5
-60+120	4.59±.02	12812±312	663±17
-120+200	5.62±.06	11487±179	878± 9
-200	4.78±.05	7493±202	725± 5

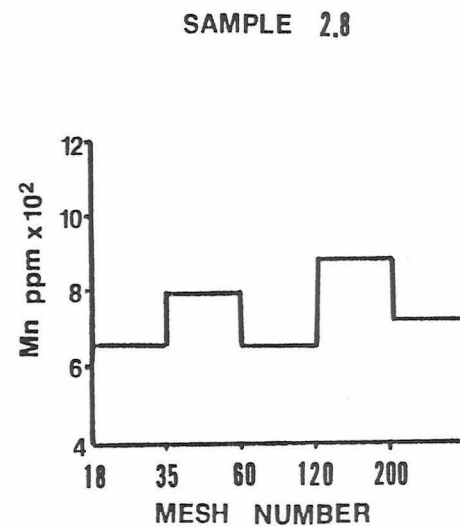
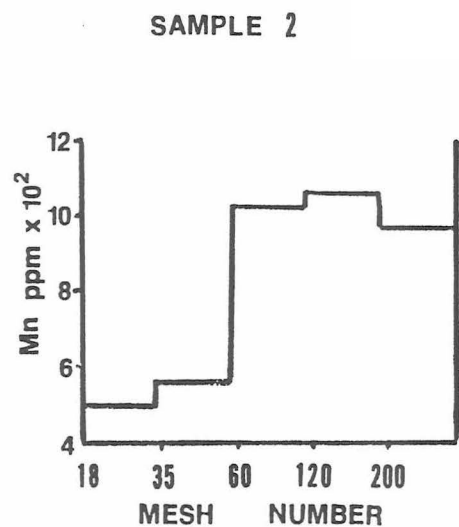
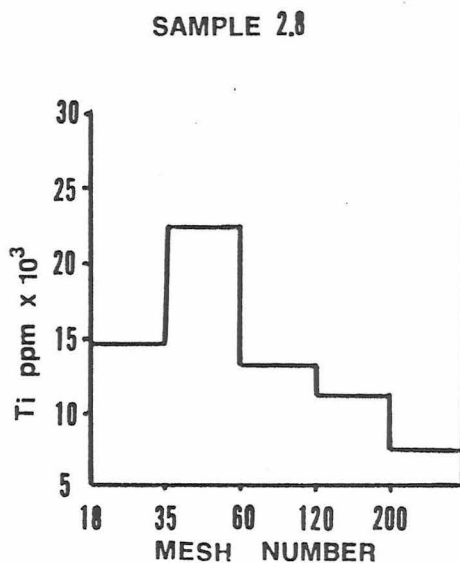
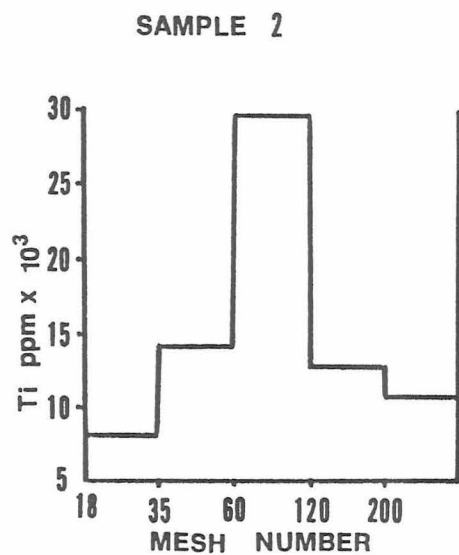
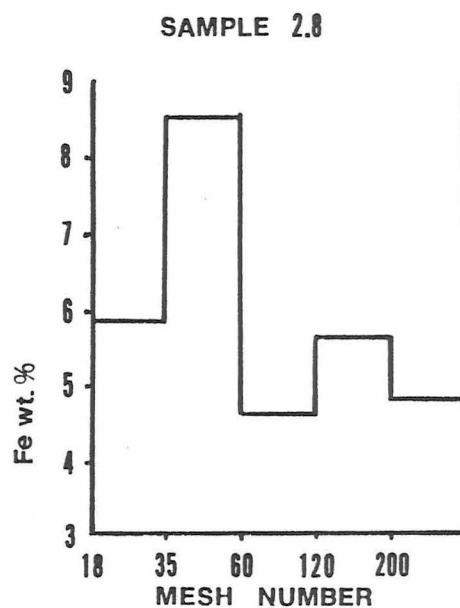
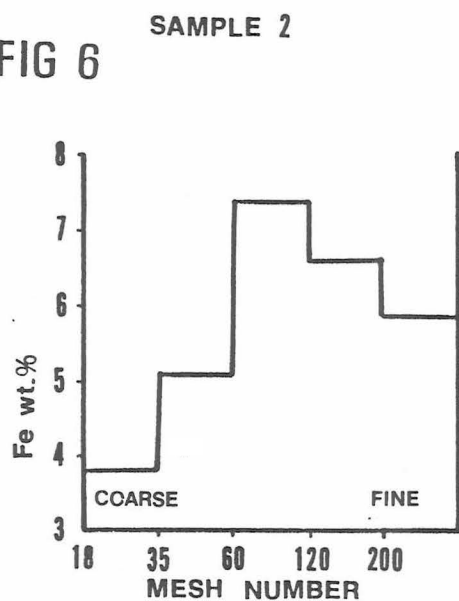
Results

Table 3-1 indicates that the concentration of all of the ore minerals within the coarser size fractions actually increase with distance. This situation presents a problem in that D comes out to be a negative number. Could it be that there is another deposit to the south producing this increase? If so, then why isn't there an increase in the finer size fractions? In order to answer this questions a plot of concentration vs mesh size was constructed for each element (See figure 6). In order to understand these diagrams, it is necessary to review the mineralogy of the deposit. The Sanford Hill deposit is composed principally of magnetite and ilmenite, while the surrounding rock is composed principally of plagioclase. Magnetite and ilmenite both lack cleavage while Plagioclase has perfect cleavage on (001) and good cleavage of (010). While the hardnesses of these minerals are nearly the same, the difference in cleavability between the ore and the anorthosite is important. Given equal hardnesses, a mineral that exhibits cleavage should be easier to grind than one that does not. If the head of the anomaly can be considered to be the zone in which material is transported basally as proposed by Stobel and Faure (1987), then both ore material and plagioclase grains would have been subjected to active grinding. Since plagioclase is easier to grind than magnetite and ilmenite, it follows that the ore minerals should retain a coarser grain size for a greater distance than the plagioclase.

Returning to figure 6 it can be seen that this is indeed the case. Notice that the -18+35 and -35+60 mesh fractions increase from sample 2 to 2.8 while the -60+120, -120+200 and -200 fractions decrease. This differential grinding effect acts to mask the "true" geochemical

Figure 6. Concentration of Fe, Ti, and Mn vs grain size for the samples within the head of the anomaly.

FIG 6



profile. To determine this, the size fractions values for samples 2 and 2.8 and those for a sample 10.6 Km down valley (sample 8) listed in table 4-1 and Appendix B were converted to bulk till values and are reported in table 4-2.

Table 4-1 Average Fe, Ti, and Mn concentrations for each size fractions of till from the Sanford Lake area N.Y.

Sample 8			
<u>Size Fraction</u>	<u>Fe (wt. %)</u>	<u>Ti (ppm)</u>	<u>Mn (ppm)</u>
-18+35	3.70±.01	8143±183	536±1
-35+60	3.42±.01	8607±101	475±7
-60+120	5.27±.01	16331±210	817±32
-120+200	5.58±.01	11174±73	896±18
-200	4.79±.02	8572±54	773±8

Table 4-2 Average Fe, Ti, and Mn concentrations within the bulk till for samples 2, 2.8, and 8.

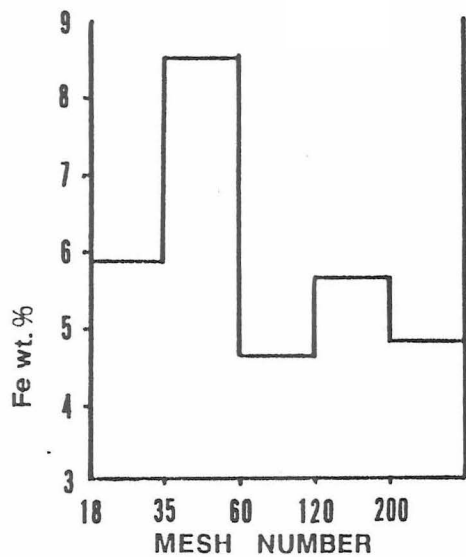
<u>Element</u>	<u>Sample 2</u>	<u>Sample 2.8</u>	<u>Sample 8</u>
Fe	5.73%	3.58%	4.56
Ti	1.60%	1.41%	1.37
Mn	.08%	.07	.07

The values in table 4-2 were obtained by multiplying the concentrations of the size fractions listed in tables 3-1 and 4-1 by the corresponding mass of that fraction for each sample. This value was then divided by the total mass of the sample. From table 4-2 it can be seen that there is still a head and a tail, but the transition can not be determined with accuracy unless more samples are analyzed.

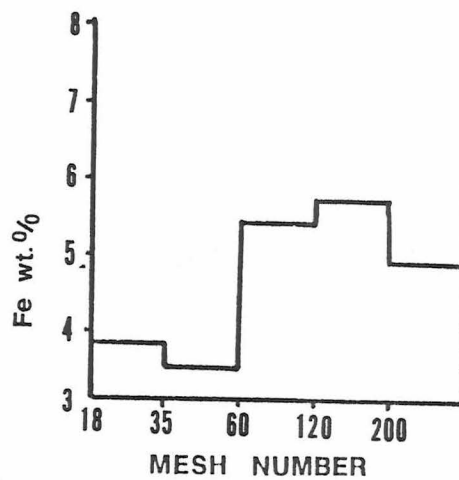
In order to determine how the ore for the different size fractions behave within the tail of the anomaly, the values listed in table 4-1 were plotted vs mesh size and compared to the plots for sample 2.8 (See

Figure 7. Concentrations of Fe, Ti, and Mn vs grain sized for two samples within the tail of the anomaly.

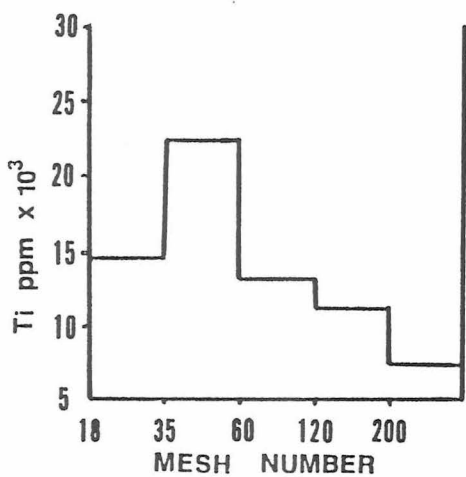
FIG 7 SAMPLE 2.8



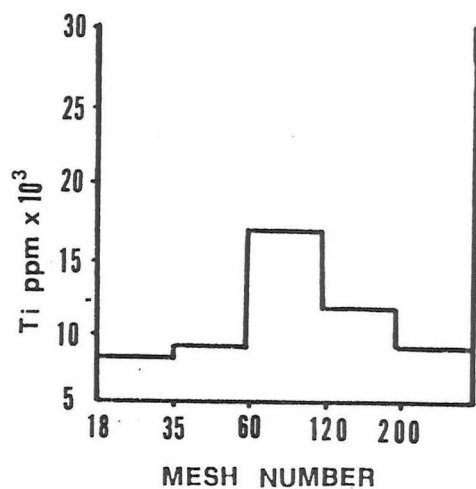
SAMPLE 8



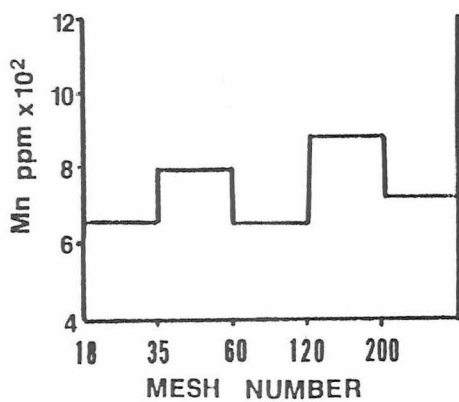
SAMPLE 2.8



SAMPLE 8



SAMPLE 2.8



SAMPLE 8

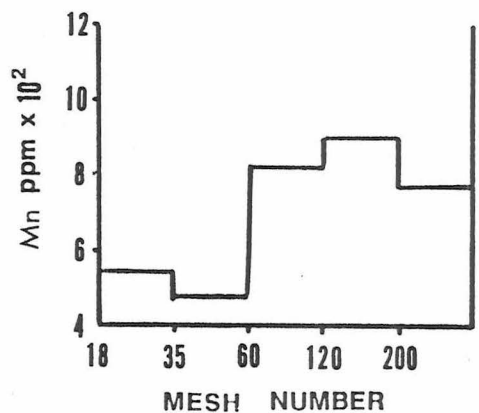


figure 7). From this figure it can be seen that the coarse grains of ore minerals are ground to the finer grain size. If the tail can be assumed to be produced by englacial transport of the ore material, then how can grinding have occurred? Apparently the ore material eventually reaches the base of the glacier due to melting of the ice. At the base, the ore grains are ground and either deposited or re-entrained into the ice sheet.

Conclusions

While it is beyond the scope of this study to prove that an exponential relationship exists south of the Sanford Hill titanomagnetite deposit I believe that this is implied. From figures 3, 4, and 5 it can be seen that there is a head and a tail within the anomaly for the -60+120 till fraction. Table 4-2 shows that the bulk till samples exhibit a similar anomaly. If in general, the head can be assumed to represent an exponential decrease then in an indirect way such a relationship can apply to the Sanford Hill deposit.

The finding that differential grinding is taking place within the head indicates that bulk till samples should be analyzed in order to average out the relative shifts in grain size. Future studies of this type on other ore types could prove to be valuable not only in the development of new explorations strategies, but also by extending our knowledge of the processes involved in the entrainment, transportation and deposition of sediment by ice sheets.

Appendix A1 Corrected concentrations of Fe O (wt%) for each run, mean values and correction coefficients for the -60+120 mesh fraction of till

Sample	1st run	2nd run	3rd run	<u>M ± 1σ</u>
1	8.591	8.695	8.582	8.623±.029
2	10.539	10.683	10.558	10.593±.037
2.8	6.517	6.638	6.553	6.569±.029
2.9	6.212	6.170	6.126	6.169±.020
3.0	18.021	18.185	18.036	18.080±.043
3.1	4.960	5.010	4.990	4.987±.012
3.2	6.628	6.650	6.553	6.610±.024
4	7.446	7.464	7.375	7.428±.022
4A	5.734	5.810	5.686	5.743±.030
5	7.945	7.957	7.971	7.958±.006
6R	7.207	7.189	7.194	7.197±.004
6G	4.519	4.557	4.545	4.540±.009
7	9.061	9.140	9.057	9.086±.022
8	7.581	7.545	7.501	7.542±.019
correction factor (f)	1.006	1.006	.997	

Appendix A2 Corrected concentrations of Mn (ppm) for each run, mean values and correction coefficients for the -60+120 mesh fraction of till.

<u>Sample</u>	<u>1st run</u>	<u>2nd run</u>	<u>3rd run</u>	<u>M ± σ</u>
1	792.61	810.27	770.34	791.00 ± 9.43
2	1023.88	1066.60	1006.47	1032.32 ± 14.58
2.8	678.89	688.55	622.62	663.35 ± 16.78
2.9	693.90	715.04	635.12	681.35 ± 19.52
3	2083.49	2101.32	2070.95	2085.29 ± 7.20
3.1	520.73	625.28	477.16	541.01 ± 35.88
3.2	695.82	709.04	635.13	680.00 ± 18.58
4	676.16	821.92	822.50	773.53 ± 39.75
4A	661.74	658.21	567.81	629.25 ± 25.10
5	888.91	913.51	889.06	897.11 ± 6.67
6R	598.90	725.26	718.74	680.97 ± 33.54
6G	455.10	562.33	475.48	497.64 ± 26.84
7	912.84	927.26	919.53	919.88 ± 3.40
8	858.35	852.79	739.30	816.81 ± 31.67
(f)	.995	1.03	.97	

Appendix A3 Corrected concentrations of Ti (ppm) for each run, mean values and correction coefficients for the -60+120 mesh fraction of till.

<u>Sample</u>	<u>1st run</u>	<u>2nd run</u>	<u>3rd run</u>	<u>M ± 1 σ</u>
1	21933.92	21195.59	22638.66	21922.73±340.17
2	29855.56	28084.87	31259.22	29733.22±749.87
2.8	12685.92	12223.76	13527.76	12812.48±311.67
2.9	13290.21	12778.30	13085.27	13051.26±121.46
3.0	37329.91	36381.15	38730.71	37480.59±557.20
3.1	7198.37	7565.85	7809.10	7524.44±144.99
3.2	12038.03	12077.54	14051.76	12722.44±543.77
4	16207.32	15709.54	17002.85	16306.57±307.52
4A	10489.09	10299.70	10408.26	10399.02± 47.80
5	15727.56	14992.01	16075.90	15598.49±260.85
6R	13707.79	14051.36	15098.63	14285.93±341.52
6G	6394.26	5816.39	6679.10	6296.58±207.22
7	23103.18	22545.04	23618.41	23088.88±253.06
8	16370.79	15867.93	16757.03	16331.92±210.16
(f)	.93	.88	.95	

Appendix A4 Concentrations of Cr (ppm) for each run and mean values for the -60+120 mesh fraction of till.

<u>Sample</u>	<u>1st run</u>	<u>2nd run</u>	<u>3rd run</u>	<u>M \pm 6</u>
1	40.57	20.55	68.50	43.21 \pm 11.35
2	55.20	64.89	56.75	58.95 \pm 2.45
2.8	66.98	67.34	92.74	75.68 \pm 6.96
2.9	41.09	46.71	71.36	53.05 \pm 7.58
3	59.57	72.75	89.37	73.89 \pm 7.04
3.1	.70	35.36	30.34	22.13 \pm 8.83
3.2	45.22	62.43	25.75	44.46 \pm 8.65
4	70.84	55.76	34.87	53.82 \pm 8.51
4A	17.00	46.86	46.86	36.91 \pm 8.12
5	53.95	38.00	73.23	64.23 \pm 3.54
6R	63.76	56.96	71.96	64.23 \pm 3.54
6G	45.17	2.51	15.20	20.96 \pm 10.32
7	68.07	15.13	63.21	48.81 \pm 13.79
8	13.84	28.34	36.86	26.35 \pm 5.48

Note - Due to the low concentration of Cr in AGV-1 the values were not corrected.

Appendix B1 Corrected concentrations of Fe_2O_3 (wt. %) for each run, mean values and correction coefficients for samples 2 and 2.8.

Sample 2				
Size Fraction	1st run	2nd run	3rd run	$M \pm \sigma$
-18+35	5.27	5.33	5.30	$5.52 \pm .18$
-35+60	7.40	7.20	7.31	$7.31 \pm .05$
-60+120	10.54	10.68	10.56	$10.60 \pm .04$
-120+200	9.53	9.47	9.38	$9.46 \pm .03$
-200	8.51	8.47	8.38	$8.45 \pm .03$
(f)	1.13	1.12	1.12	
Sample 2.8				
-18+35	8.21	8.23	8.38	$8.28 \pm .04$
-35+60	11.82	12.18	12.32	$12.10 \pm .12$
-60+120	6.52	6.64	6.55	$6.57 \pm .03$
-120+200	7.98	7.89	8.26	$8.04 \pm .09$
-200	6.74	6.75	7.02	$6.84 \pm .07$
(f)	1.11	1.11	1.14	
Sample 8				
-18+35	5.29	5.28	5.30	$5.29 \pm .01$
-35+60	4.87	4.93	4.90	$4.90 \pm .01$
-60+120	7.58	7.54	7.50	$7.54 \pm .02$
-120+200	7.97	7.99	7.97	$7.98 \pm .01$
-200	6.93	6.93	6.78	$6.86 \pm .04$
(f)	1.13	1.12	1.12	

Appendix B2 Corrected concentrations of Mn (ppm) for each run, mean values and correction coefficients for till samples 2, 2.8, and 8.

Sample 2				
<u>Size Fraction</u>	<u>1st run</u>	<u>2nd run</u>	<u>3rd run</u>	<u>M ± s</u>
-18+35	493.78	518.40	482.61	498.24 ± 8.63
-35+60	579.71	554.84	556.94	563.83 ± 6.50
-60+120	1023.88	1066.60	1006.47	1032.32 ± 14.58
-120+200	1044.54	1107.30	1027.46	1059.77 ± 34.33
-200	968.82	1001.20	951.42	973.81 ± 11.91
(f)	1.08	1.09	1.03	
Sample 2.8				
-18+35	651.74	689.02	654.95	665.24 ± 9.74
-35+60	804.98	788.95	809.70	801.21 ± 5.13
-60+120	678.89	688.55	622.62	663.35 ± 16.78
-120+200	899.62	872.74	862.92	878.43 ± 8.96
-200	727.87	734.93	713.03	725.28 ± 5.27
(f)	1.09	1.09	1.07	
Sample 8				
-18+35	538.50	534.83	535.97	536.43 ± 0.88
-35+60	458.83	490.59	476.59	475.24 ± 7.44
-60+120	858.35	852.79	739.30	816.81 ± 31.67
-120+200	902.70	931.96	854.03	896.23 ± 18.56
-200	765.65	792.93	761.90	773.49 ± 7.98
(f)	1.08	1.09	1.03	

Appendix B3 Corrected concentrations of Ti (ppm) for each run, mean values and correction coefficients for till samples 2, 2.8 and 8.

Sample 2

<u>Size Fraction</u>	<u>1st run</u>	<u>2nd run</u>	<u>3rd run</u>	<u>M ± s</u>
-18+35	8075	8245	8439	8253±85
-35+60	13585	13774	13725	13694±46
-60+120	29855	28084	31259	29733±749
-120+200	12635	12901	12513	12683±93
-200	10165	10573	10961	10566±187
(f)	.95	.97	.97	

Sample 2.8

-18+35	13972	14770	14870	14537±232
-35+60	22655	22954	21457	22355±373
-60+120	12685	12223	13527	12812±312
-120+200	11776	11627	11057	11487±179
-200	7186	7984	7309	7493±202
(f)	.998	.998	.937	

Sample 8

-18+35	7695	8390	8342	8143±183
-35+60	8360	8730	8730	8607±101
-60+120	16370	15867	16757	16331±210
-120+200	11115	11349	11058	11174±73
-200	8645	8633	8439	8572±54
(f)	.95	.97	.97	

Appendix B4 Concentrations of Cr (ppm) for each run and mean values for till samples 2, 2.8, and 8.

Sample 2

<u>Size Fraction</u>	<u>1st run</u>	<u>2nd run</u>	<u>3rd run</u>	<u>M ± σ</u>
-18+35	8.79	61.25	27.91	32.65±12.51
-35+60	30.93	64.95	56.50	50.79±8.35
-60+120	55.20	45.02	56.76	58.95±2.45
-120+200	23.74	48.15	32.75	33.84±5.03
-200	2.15	6.85	57.37	35.89±13.94

Sample 2.8

-18+35	86.97	113.53	96.57	99.02±6.34
-35+60	150.58	152.51	114.56	139.21±10.08
-60+120	66.98	67.34	92.74	75.69±6.96
-120+200	49.77	67.27	53.78	56.94±4.32
-200	44.12	37.48	53.34	44.98±3.76

Sample 8

-18+35	5.09	16.84	- 5.91*	5.34±5.36
-35+60	53.56	- 10.10*	44.63	31.03±16.82
-60+120	13.85	28.35	36.87	26.35±5.49
-120+200	60.52	32.20	11.05	34.61±11.71
-200	6.14	8.25	33.25	15.88±7.11

*Note - Negative values result from the inaccuracy of the analysis and the low Cr concentration in the till.

Acknowledgements

I would like to thank Dr. G. Faure for his constant support and encouragement during the course of this study. In addition, special thanks are due to Cindy Whiting for the typing of the manuscript.

References

- Anonymous, 1967, Titaniferous Ores of the Sanford Lake District, New York: in Ore Deposits of the United States, 1933-1967. p141-153.
- Dreimanis, A and Vagners, U.J 1971: Bimodal distribution of rock and mineral fragments in basal tills: In Goldthwait, R.P (ed) Till: A Symposium, Columbus Ohio State University Press, p 237-250.
- Kauranne, L.K., ed. 1976, conceptual models in exploration geochemistry, Norden 1975: Jour. Geochem. Explor., v.5, p 173-410.
- Kays, M.A., 1965, Petrographic and modal relations, Sanford Hill titaniferous magnetite deposit: Econ. Geol. v.60, p 1261-1297.
- Shilts, W.W., 1973 Glacial dispersal of rocks, minerals, and trace elements in Wisconsinan till, southeastern Quebec, Canada: Geol. Soc. America Mem. 136 p189-219.
- Strobel, M.L. and Faure, G, 1987 Transport of indicator clasts by ice sheets and the transport half-distance: A contribution to prospecting for ore deposits: Jour. of Geol. v.95, p 687-697.
- Walton, M and De Waard, D, 1962, Orogenic and stratigraphic development of the Precambrian in the Adirondack Highlands: Abstract, Geol. Soc. America Spec. Paper 73, p 258.